

Highly Selective Artificial K⁺ Channels: An Example of Selectivity-Induced Transmembrane Potential

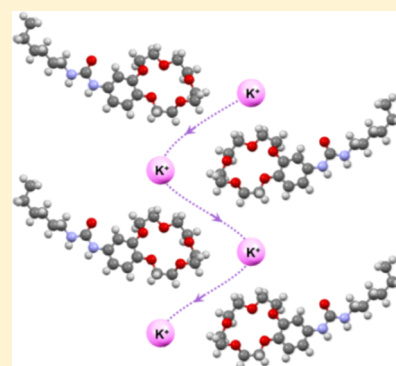
Arnaud Gilles[†] and Mihail Barboiu^{*,†,‡}

[†]Adaptive Supramolecular Nanosystems Group, Institut Européen des Membranes, ENSCM-UMII-CNRS UMR-5635, Place Eugène Bataillon, CC 047, F-34095 Montpellier, France

[‡]MOE Laboratory of Bioinorganic and Synthetic Chemistry, Lehn Institute of Functional materials, School of Chemistry and Chemical Engineering, Sun Yat-Sen University, Guangzhou 510275, China

S Supporting Information

ABSTRACT: Natural KcsA K⁺ channels conduct at high rates with an extraordinary selectivity for K⁺ cations, excluding the Na⁺ or other cations. Biomimetic artificial channels have been designed in order to mimick the ionic activity of KcsA channels, but simple artificial systems presenting high K⁺/Na⁺ selectivity are rare. Here we report an artificial ion channel of H-bonded hexyl-benzoureido-15-crown-5-ether, where K⁺ cations are highly preferred to Na⁺ cations. The K⁺-channel conductance is interpreted as arising in the formation of oligomeric highly cooperative channels, resulting in the cation-induced membrane polarization and enhanced transport rates without or under pH-active gradient. These channels are selectively responsive to the presence of K⁺ cations, even in the presence of a large excess of Na⁺. From the conceptual point of view, these channels express a synergistic adaptive behavior: the addition of the K⁺ cation drives the selection and the construction of constitutional polarized ion channels toward the selective conduction of the K⁺ cation that promotes their generation in the first place.



INTRODUCTION

Ion and water–protein channels are involved in important fundamental physiological processes such as nerve influx, muscular contraction, and metabolite neuronal exchange.¹ They control the electrical and chemical exchanges between intra- and extracellular medium, by allowing the facilitated diffusion of ionic or polar species through the membrane. These proteins are usually gated and respond to external stimuli, such as osmotic and pH gradients, and even, for few of them, to light.² Structural effects exerted by the macrodipolar orientation of protein fragments within active biological pores may supplementary contribute to the selectivity of potassium, chloride, proton and water translocation.^{3–6} Highly selective natural channels inevitably lead to stable membrane potentials. Valinomycin (a carrier) has been used this way for some time.¹ The fact that most reported artificial systems cannot achieve this type stable potential suited to drive other gradients is simply due to their poor selectivity. Despite their tremendous importance in natural protein channels, high-selectivity issues have been rarely described as determinant for the transport performances of artificial biomimetic systems.^{7–12} Indeed, such synthetic ion channels, with gating and selectivity properties, made of less complicated structures than that of proteins, opened new ways toward the understanding of complex phenomena related ionic translocation through artificial biomimetic channels.^{13–19}

Among these artificial systems, the macrocyclic crown ethers have already been studied as ion translocators in bilayer

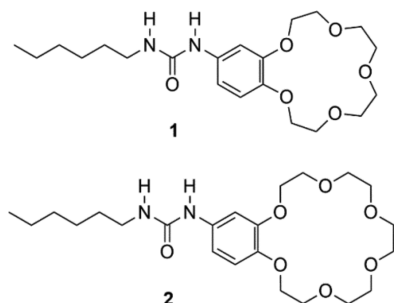
membranes. We have already developed H-bonded self-assembled ion channels incorporating crown ethers where the ion-translocation functions are dynamically associated with supramolecular channels^{19–21} and materials.^{22–24} Previous studies demonstrated that significant membrane disruption is observed for alkyl-benzoureido-crown-ethers, showing clear regular channel activities.¹⁹ Within this context we presumed that the entropic cost of cation dehydration must be strongly optimal in the case where the macrocycle of the receptors is dimensionally compatible with the diameter of cations, for example, Na⁺ with 15-crown-5-ether and K⁺ with 18-crown-6-ether. The hexyl-benzoureido-15-crown-5-ether **1** and hexyl-benzoureido-18-crown-6-ether **2** possess the ability to form columnar self-assembled ion channels within lipid bilayers, showing an extremely complex set of conductance levels for fittest Na⁺ and K⁺, respectively, depending on their concentration in the bilayer membrane.¹⁹

In order to get new mechanistic insights on supramolecular assembled ion channel functions and to assess their ion selectivity, we serendipitously found that the hexyl-benzoureido-15-crown-5-ether **1** is able to slowly transport smaller Li⁺ and fittest Na⁺ cations, while, and in a very interesting manner, the K⁺, Rb⁺, Cs⁺ cations with diameters bigger than a 15-crown-5 macrocycle are transported with higher transport rates even in the absence of a transmembrane pH gradient, which is

Received: November 13, 2015

Published: December 21, 2015

usually a prerequisite to initiate proton/cation antiport translocation through the lipid bilayer.²⁰ Surprisingly, together with this unexpected result, we found herein another phenomenon: The passive carrier-induced influx of K^+ , Rb^+ , Cs^+ cations generates a membrane polarization that induced a quite stable transmembrane potential modification unprecedentedly observed for this artificial ion-channel system.



RESULTS AND DISCUSSION

To evaluate the transport of the alkali cations with ascending concentration of compound **1**, we first designed the experiment as follows: EYPC liposomes [large unilamellar vesicles (LUV), 100 nm diameter] were filled with a pH-sensitive dye (HPTS) and 100 mM NaCl in a phosphate buffer solution (10 mM, pH 6.4). The liposomes were then suspended in an external phosphate buffer solution (10 mM, pH 6.4) containing 100 mM of NaCl or KCl. Then, after introduction of **1**, an external pH gradient was created by addition of NaOH. The internal pH change inside the liposome was then monitored by the change in the fluorescence of HPTS. For each batch of experiments, a blank experiment in the absence of **1** was recorded, to evaluate simple diffusion through the liposome bilayer. We calculated the first-order initial rate constant from the slopes of the plot of $\ln([H^+]_{in} - [H^+]_{out})$ versus time, where $[H^+]_{in}$ and $[H^+]_{out}$ are the intravesicular and extravesicular proton concentrations, respectively. The $[H^+]_{out}$ was assumed to remain constant during the experiment (pH 7.4), while $[H^+]_{in}$ values were calculated for each point from HPTS emission intensity using the equation $pH = 1.1684 \times \log(I_{460}/I_{403}) + 6.9807$. From these experiments, it appeared clearly that the conductance behaviors are highly different depending on the nature of the alkali cation on the outside of the vesicle. Indeed, when tested with NaCl on external buffer, the ion channel had the expected behavior: After the compound **1** injection at $t = 60$ s, the internal pH remains quasi-stable and only the creation of a pH gradient, applied at $t = 300$ s, induces the increase of the internal pH, reminiscent with the Na^+ influx (Figure 1a).

A contrario, the same experiment performed with KCl, instead of NaCl in the external buffer, shows a completely different behavior (Figure 1b): At the beginning of the experiment, at $t = 0$ s, the internal pH remains stable.

The addition of **1** at 60 s generates a rapid increase of the internal pH, followed by a slow diminution after ca. 100 s. After 500 s, the external pH is modified by addition of NaOH to get an external pH at ca. 7.4. Immediately, a more abrupt increase of pH inside the vesicle indicated a faster efflux of proton than previously observed for Na^+ and, consequently, a higher influx rate for K^+ . A slow and slight decrease of internal pH then occurred, before lysis of the vesicle (900 s).

Thus, from these first experiments it appears evident that the ion-channel behaviors are highly dependent on the nature of

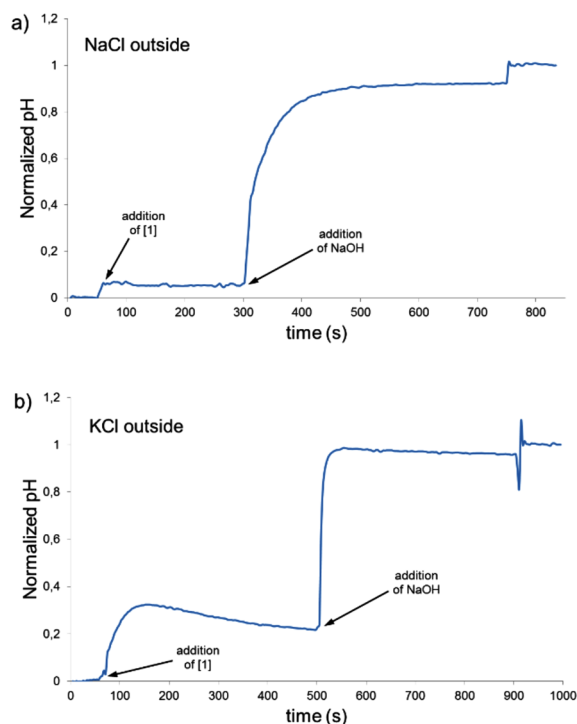


Figure 1. Time dependence of normalized internal pH of LUV of internal composition of 100 mM NaCl and 10 μ M HPTS in 10 mM phosphate buffer at pH 6.4 and external compositions of (a) 100 mM NaCl or (b) KCl in 10 mM in phosphate buffer at pH 6.4 on the addition of **1** (200 μ M final concentration) in the bilayer membrane at $t = 50$ s and of NaOH in the external compartment at $t =$ (a) 300 s and (b) 500 s. For a better viewing, starting and final internal pH have been normalized from 0 to 1 for each experiment. Also, for each different cation, a blank experiment has been done, showing no pH modification in absence of **1** (not shown).

the cation. The K^+ cation induces a specific organization of the ion channels within membrane behaving polarization behaviors. They kinetically transport faster under the pH gradient the K^+ cations created in these responsive K^+ -channels the first time. Experiments have also been done for compound **2**. Dose-response graphs show the same type of behavior as that of compound **1**. On the contrary to compound **1**, this behavior was expected since it is now well-known that 18-crown-6-ether has more affinity toward K^+ . However, these experiments also clearly show that the transport activity of **1** remains much higher than **2** (see Supporting Information (SI)). We thus decided to stay focused on compound **1** that shows the most interest.

We then tested the transport conductance states of channels of **1** with increasing ionophore concentration, with NaCl inside and NaCl (Figure 2a) or KCl (Figure 2b) outside the vesicles for which the associated pseudo-first order initial kinetic constant rates have been determined (Figure 2c).

The analysis of the pseudo-first-order kinetic initial rates of the cation transport through the channels as a function of the concentration of **1** into bilayer membrane reveals a polynomial (almost linear) and a sigmoidal fit of concentration-activity relationship for the Na^+ and K^+ cations, respectively (Figure 2c). These results show that compound **1** forms highly cooperative ion channels toward K^+ cations with a saturation behavior at 150 μ M of **1** in the bilayer and presents a much lower activity for Na^+ cations where the plateau is not attained

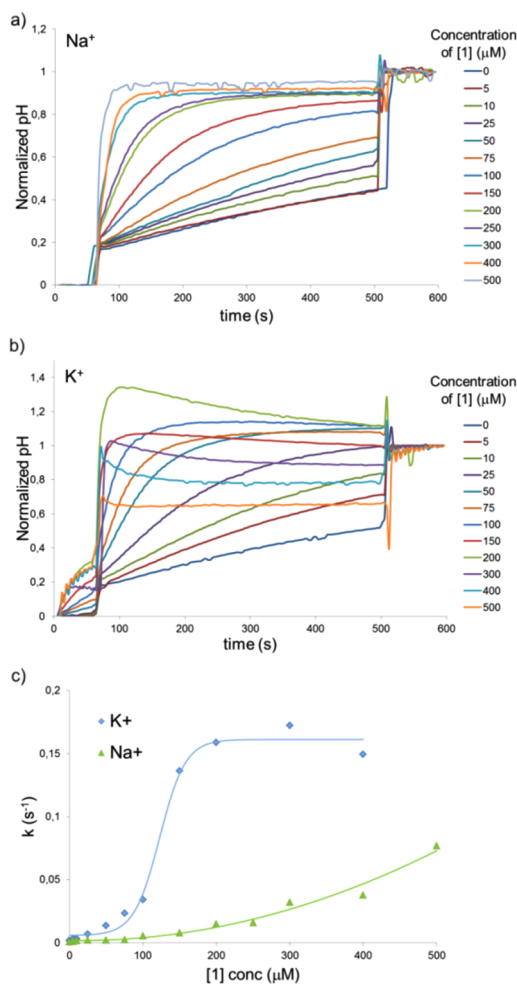


Figure 2. Normalized pH (see SI) change inside LUV as a function of time for (a) Na⁺ and (b) K⁺ transport at different concentrations of **1** in the bilayer membrane. Internal composition of LUV is 100 mM NaCl, 10 mM phosphate buffer at pH 6.4, and HPTS 10 μM. External compositions are 100 mM (a) NaCl or (b) KCl in 10 mM phosphate buffer at pH 6.4. (c) Pseudo-first-order initial constant rate as a function of final concentration of **1** in the bilayer membrane.

before the limit of solubility of **1** for which precipitation occurs at 500 μM. Under the same conditions, compound **1** (150 μM) presents a 1 order of magnitude higher initial transport rate of $k_{K^+} = 0.156 \text{ s}^{-1}$ for K⁺ cations and $k_{Na^+} = 0.015 \text{ s}^{-1}$ for Na⁺, with kinetic selectivity of $S_{K^+/Na^+} = 3\text{--}17$, depending on the concentration.

To gain more insight on cations conductance behaviors, a Hill analysis was performed. After determination of fractional activity (*Y*) at 500 s (see SI) for each concentration, we plotted *Y* versus log[concentration of **1**] for K⁺ and Na⁺ (Figure 3). The logistic function obtained can be fitted with the two-parameter Hill equation $Y = 1/(1 + (EC_{50}/[C])^n)$, providing EC₅₀ (the effective monomer concentration needed to reach 50% activity) and Hill coefficient (*n*): EC₅₀(Na⁺) = 74 μM, EC₅₀(K⁺) = 10 μM; $n_{Na^+} = 1.63$, $n_{K^+} = 1.66$. The EC₅₀ for K⁺ is almost 1 order of magnitude smaller than for Na⁺. Despite the remarkable difference in transport activity, the Hill coefficients for both cations are the same, reminiscent with the formation of class I channels ($n > 1$) of similar supramolecular constitution, which correspond to more than one active molecule forming the channel superstructure. We can thus assume that self-

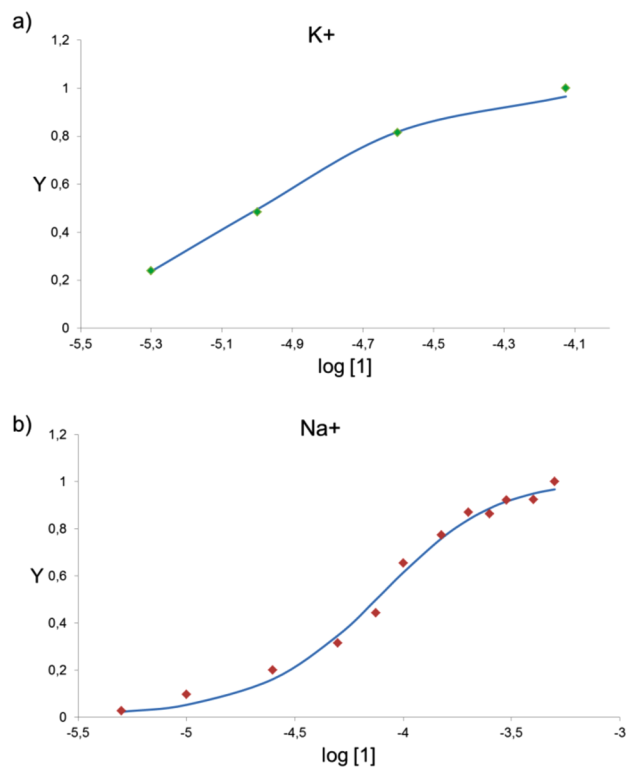


Figure 3. Fractional activity $Y = f(\log[1])$ plotted for (a) Na⁺ and (b) K⁺ cations. Solid circles (●) are experimental data, and the curves are the best calculated fit from the Hill equation.

assembly of the channel does occur within the bilayer, and not by incorporation of a preassembled channel which corresponds to more than one molecule of **1** binding the cations within bilayer membrane.²⁰

The difference between the cation-induced self-organization of supramolecular ion channels of **1** and the polarization of the bilayer membranes rationalizes, in part, for the very low transport activity of the smaller Li⁺ and fittest Na⁺ cations, while the bigger K⁺, Rb⁺, and Cs⁺ cations show passive transport conductance states in the absence of pH gradient (Figure 4). Interestingly, this passive activation occurs only if a cation concentration gradient is established between intra- and extravesicular media. No passive activation is observed with equal concentrations of KCl inside and the outside of the vesicle. More interestingly, when KCl is present inside the vesicle, the passive activation of the transport is reversed, and the pH gradient generated transport follows the same trend as previously observed (Figure 4). It is noteworthy that in this case, K⁺ also has better transport rates than Rb⁺ and Cs⁺ cations.

For the alkali cations, the transport activity increases in the order $Li^+ \cong Na^+ \ll K^+ \cong Rb^+ \cong Cs^+$, following the Eisenman sequence I corresponding to the energetic penalty for ions dehydration (Figure 5a).²¹ We identified two sets of activity with an important gap of conductance states between Na⁺ and K⁺, reminiscent with the constitutional ion-channel reorganization behaviors in the presence of cations bigger than the 15-crown-5 macrocyclic cavity (Figure 5b).

Next, it would be essential to know if the passive activation behavior is cation concentration dependent and if it is considered a dynamic reversible process. Thus, in a new experiment, with 100 mM NaCl inside and outside the vesicle,

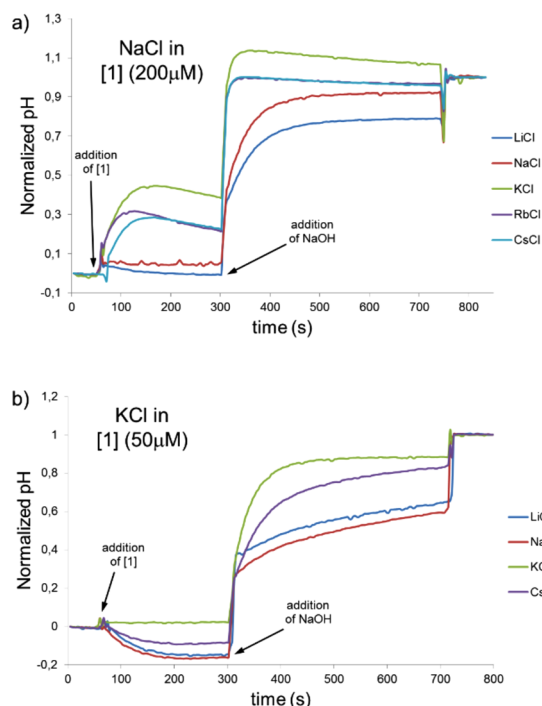


Figure 4. Time dependence of normalized internal pH of LUV of internal composition of (a) NaCl and (b) KCl and external composition of 100 mM MCl, $M^+ = \text{Li}^+, \text{Na}^+, \text{K}^+, \text{Rb}^+, \text{Cs}^+$. **1** ($200 \mu\text{M}$ (a) and $50 \mu\text{M}$ (b) final concentrations) was injected at $t = 60$ s and 0.5 M NaOH solution at $t = 300$ s. Maximum pH was reached after lysis with 5% triton X100 ($40 \mu\text{L}$). For a better viewing, starting and final internal pH have been normalized from 0 to 1 for each experiment. Also, for each different cation, a blank experiment has been done, showing no pH modification in absence of **1**.

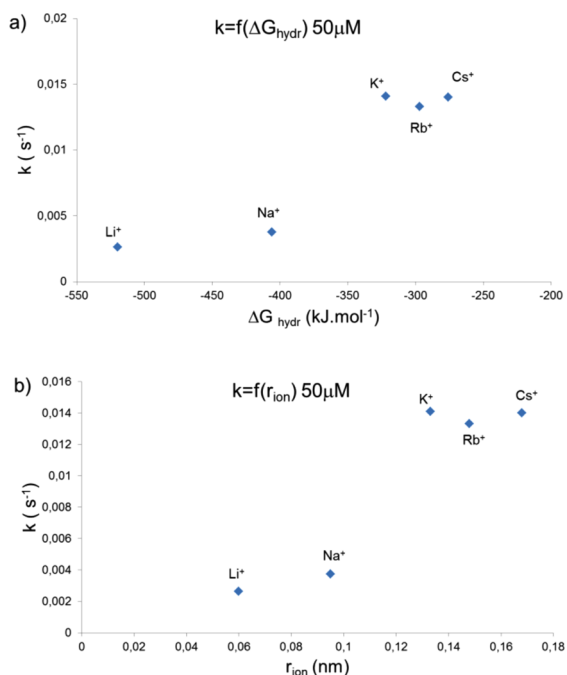


Figure 5. Initial constant rates of various cations as a function of hydration free enthalpy or radius of cation for $50 \mu\text{M}$ of **1**.

after addition of the compound **1** ($200 \mu\text{M}$) in the bilayer membrane, no noticeable pH change occurs, nor after addition of supplementary external 100 mM NaCl (thus creating an

osmotic gradient) (Figure 6a). Then, after addition of increasing concentrations of KCl after 400s in extravascular

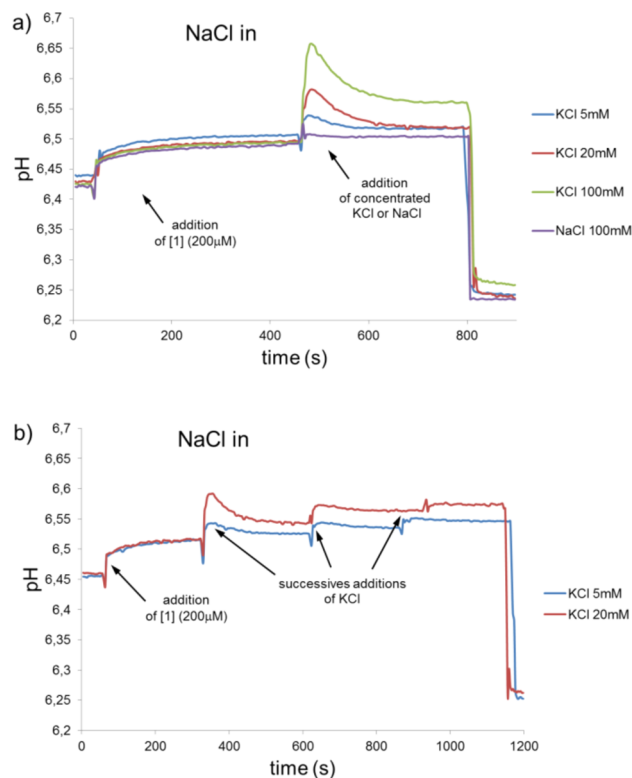


Figure 6. Channel response to in situ cation modification. Concentration indicated is the final external concentration of NaCl or KCl. Internal composition of LUV is 100 mM NaCl, 10 mM phosphate buffer at pH 6.4, and HPTS $10 \mu\text{M}$. External compositions are 100 mM NaCl and 10 mM phosphate buffer at pH 6.4 at the beginning of each experiment and are then modified by one addition of **1** ($200 \mu\text{M}$) followed by KCl or NaCl (a) or successive additions of KCl (b).

media, we observed that the passive internal pH change occurs, with an intensity proportional with the external KCl concentration. Remarkably, compound **1** is responsive to the presence of K^+ , even in the presence of a large excess of Na^+ . In this case, the driving force that generates the proton efflux is still the transmembrane potential generated by the highest permeability of K^+ through selective self-generated K^+ -channels. Then, when multiple consecutive additions of the same 5 or 20 mM solution of K^+ are made, we observe that the response is progressively lowered after the first injection (Figure 6b). This is due to the fact that the transmembrane potential generated with the first addition of K^+ is much higher compared to the following ones, due to the decrease of the K^+ concentration gradient between the intra- and extra-vesicular media with the increase of the K^+ cation concentration in the intravesicular medium.

In order to directly observe that membrane hyperpolarization occurs upon addition of **1**, we run experiments using safranin O, which is a potential sensitive dye that reports the membrane polarization.²² The results in Figure 7 show that, after a decrease of fluorescence upon addition of compound **1** in the bilayer membrane (which could be attributed to a direct interaction between Safranin O and **1**), no change in fluorescence arises with Na^+ inside, even with K^+ outside. In

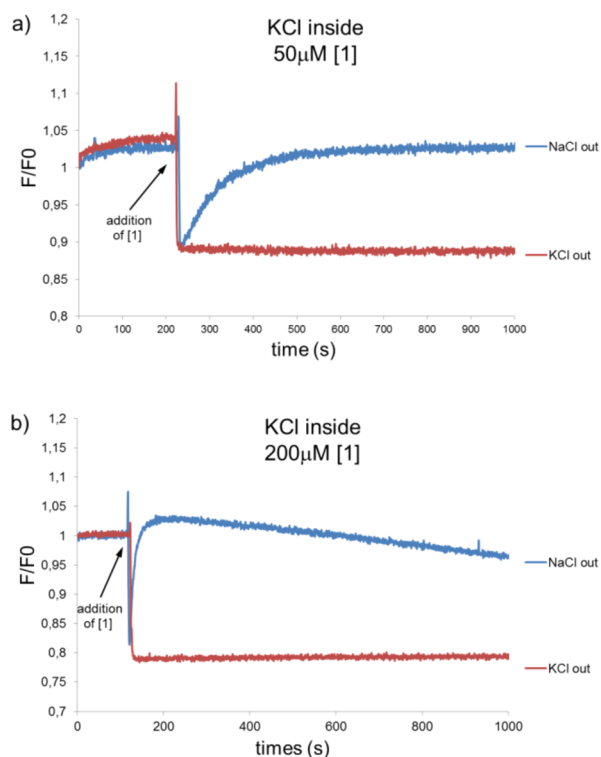


Figure 7. Membrane potential experiments with safranin O. LUV composition: KCl 100 mM and PBS pH 6.4 inside and KCl or NaCl (100 mM), PBS pH 6.4 and safranin O (60 nM) outside. Final concentrations of **1** are 50 μM (a) and 200 μM (b).

fact, since the created potential gave rise to a negative charge on the outside, this has no effect on safranin O fluorescence²³ (see SI). The same experiment performed with KCl instead of NaCl in the internal buffer clearly shows that a transmembrane potential modification occurs in a fast process when NaCl is present on the outside of the vesicle (Figure 7), due to an accumulation of positive charges on the outside of the vesicles.

Based on these experiments, we are proposing a mechanistic scenario for selective K^+ translocation under passive and active conditions. The Figure 8 below gives a representative view of this step-by-step process. The addition of compound **1** in the bilayer membrane induces a rapid specific structuration of the ion channel selectively occurring in the presence of K^+ or Rb^+ and Cs^+ cations presenting fast influx rates (we believe that channel-specific structuration arising from the interaction of **1**

with Na^+ is less effective to induce important conductance states). It generates a transmembrane potential due to accumulation of positive charges on the inside and of negative charges on the outside of the bilayer membrane (Figure 8a). The induced transmembrane potential synergistically generates a fast proton efflux in order to restore the electrical balance. The resulting effect is a temporary, quite remarkable self-pumping of K^+ cations inside the vesicle. The pH increase inside the vesicle further tends, after reaching maximum value, to revert the translocation processes. A slow Na^+/H^+ influx and K^+ efflux antiport translocations slowly re-equilibrate, against the concentration gradients, the created pH gradient (Figure 8b). A slow H^+ influx and Na^+ efflux antiport translocations slowly re-equilibrate the created pH gradient. Na^+ efflux is osmotically favored against K^+ efflux, which would be against its concentration gradient. This moreover explains why this part of the curve is much slower. After addition of NaOH in order to increase external pH to 7.4, a very fast efflux of H^+ occurs and generates a very fast antiport influx of K^+ (Figure 8c).

Interestingly, in the case of a high concentration of **1** within the membrane, the fast pH increase is enhanced by a supplementary proton efflux in such a manner that the internal pH reaches superior values to the external pH (Figure 1b and 2b).

Similar to the first part of the passive transport conditions before the addition of NaOH, the transmembrane potential is activating a supplementary proton efflux reaching a maximal pH_{in} value thus independent of the pH gradient, followed by slow proton influx to re-equilibrate the pH (Figure 8d).

We know from previous studies by us or others that hexylureido-benzo-15-crown-5-ether recognizes the Na^+ via the equatorial binding of the cation by the oxygens of the macrocycle moiety.^{24–28} However, the oxygen binding sites of the crown-ether moiety are not completely covering the apical hydration sites of Na^+ , so its dehydration is not completely compensated. Differently in the sandwich-type geometry observed for complexation of the bigger K^+ cations by two 15-crown-5-ethers, the oxygen atoms of both macrocycles are completely surrounding the K^+ cations in a similar manner to the water molecules around the hydrated cation. This is reminiscent with the KcsA K^+ natural channel binding behaviors in the active gate: The spatial positioning of the carbonyl moieties is perfectly replacing the hydration sphere of K^+ cations.²⁹ Interestingly, the 2:1 “sandwich” structures and selective effects of smaller crown-ether cavity sizes on the metal-ion/macrocycle complexation seem to be systematically

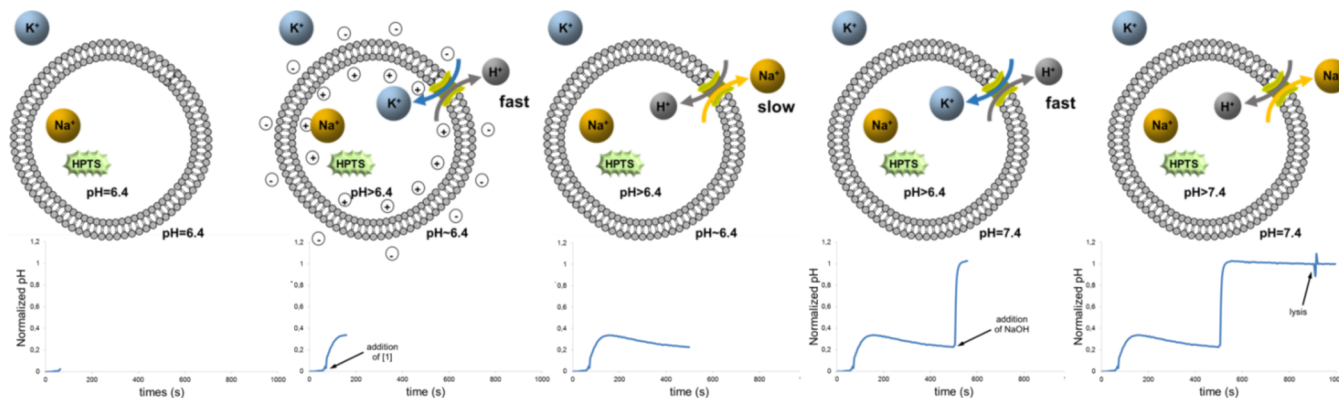


Figure 8. Schematic representation of the proposed step-by-step cation/proton translocation mechanism; see text for the details.

rationalized for recently reported K^+ -selective chromatographic,³⁰ membrane,³¹ and sensing^{32,33} polymeric systems.

The exact transport mechanism of cations across the bilayer ion channels is difficult to accurately describe by these structural data. However, it is most probably that the cations can translocate channels of self-assembled macrocyclic sites as unique cation-binding sites within the membrane environment. More sophisticated undefined pores created by crown-aggregates may be also involving macrocyclic moieties in close spatial proximity.

It was previously postulated that the cation-file diffusion is occurring as successive binding processes via macrocyclic site-to-site jumping along the crown-sites, acting as an exceptional biomimetic hydrophilic lubricant in the hydrophobic bilayer environment.^{19,33} From these studies we know that the optimal and maximum distances an ion is translocated between two individual crown-sites within a membrane environment are 6 and 11 Å, respectively.³³

The ureido-crown-ether systems presented here form ribbon-like H-bonded structures in solution, in the solid state,^{19,24} and they are most probably self-assembling multivalent macrocyclic aggregates within the bilayer membrane. From their X-ray crystal structures we know that the distance between two urea-H-bonded crown-ether neighboring sites is 4.8 Å, very close to optimal 3.3 Å distance observed in K^+ -(15-crown-5)₂ sandwich complex. The close proximity of macrocyclic binding sites favors multivalent crown-ether-cation contacts recovering the hydration sphere of the cation. This is clearly favoring the selective binding of K^+ cations, against the imperfectly coordinated Na^+ cations. The cation translocation is also related to the dynamics of the crown-ether aggregates within bilayers. We know from our previous studies that similar cholesteryl-thioureido-ethylamide-15-crown-5-ether³⁴ and squalyl-amido-benzo-15-crown-5-ether³⁵ compounds present initial transport rates for K^+ cations of $k_{K^+} = 3.9 \times 10^{-3} \text{ s}^{-1}$ and $k_{K^+} = 87.5 \times 10^{-3} \text{ s}^{-1}$, (1:10 mol:mol, compd:lipid), respectively. Under the same conditions, compound **1** presents 1 order of magnitude higher initial transport rate of $k_{K^+} = 175 \times 10^{-3} \text{ s}^{-1}$ for K^+ cations. The higher mobility hexyl-decorated compound **1** related to the cholesteryl and squalyl-SQ tails with relatively lower fluidities within bilayer membrane would favor the formation of highly dynamic and less rigid channel superstructures. They are required for the highly adaptive translocation of cations via multivalent binding/release equilibria with spatially close macrocyclic relays inside of the bilayer.

SUMMARY

In summary, by using simple ureido-15-crown-5-ether compounds self-assembling in ion channel H-bonded superstructures within bilayer membranes, we demonstrated that multivalent sandwich-type binding toward K^+ and bigger cations is responsible for their high translocation rates inducing the passive polarization of the membrane. It results in the formation of highly cooperative ion channels toward K^+ cations presenting passive activation and enhanced transport rates under a pH-active gradient. These channels are selectively responsive to the presence of K^+ cations, even in the presence of a large excess of Na^+ . Conversely, the molecular-scale dynamics of molecules within the ion channels superstructures is of crucial relevance for the observed selective biomimetic translocation, like ionic conduction in neurons.

From the conceptual point of view these channels express a synergistic adaptive behavior: The addition of the K^+ cation drives the selection and the construction of constitutional polarized ion channels toward the selective conduction of the K^+ cation that promoted its generation in the first place. This is a nice, dynamic self-instructed (“self-trained”) ion-channel system where a solute induces itself the activation of its own selective transport. We are currently exploring the use of these mixed self-assembled channels for the development of commutable or efficient ion separation switches or devices.

ASSOCIATED CONTENT

Supporting Information

The Supporting Information is available free of charge on the ACS Publications website at DOI: 10.1021/jacs.5b11743.

Materials and methods, synthetic and experimental details of LUV preparation and cation transport experiments (PDF)

AUTHOR INFORMATION

Corresponding Author

*mihail-dumitru.barboiu@univ-montp2.fr

Notes

The authors declare no competing financial interest.

ACKNOWLEDGMENTS

This work was financially supported by ANR Blanc International DYNAMULTIREC (13-IS07-0002-01)

REFERENCES

- (1) Hille, B. *Ion Channels of Excitable Membranes*, 3rd ed.; Sinauer Associates: Sunderland, MA, 2001.
- (2) Nagel, G.; Ollig, D.; Fuhrmann, M.; Kateriya, S.; Musti, A. M.; Bamberg, E.; Hegemann, P. *Science* **2002**, *296*, 2395–2398.
- (3) Doyle, D. A.; Morais Cabral, J.; Pfuetzner, R. A.; Kuo, A.; Gulbis, J. M.; Cohen, S. L.; Chait, B. T.; MacKinnon, R. *Science* **1998**, *280*, 69–77.
- (4) Dutzler, R.; Campbell, E. B.; MacKinnon, R. *Science* **2003**, *300*, 108–112.
- (5) de Groot, B. L.; Grubüller, H. *Curr. Opin. Struct. Biol.* **2005**, *15*, 176–183.
- (6) Agre, P. *Angew. Chem., Int. Ed.* **2004**, *43*, 4278–4290.
- (7) Hennig, A.; Fischer, L.; Guichard, G.; Matile, S. *J. Am. Chem. Soc.* **2009**, *131*, 16889–16895.
- (8) Barboiu, M.; Gilles, A. *Acc. Chem. Res.* **2013**, *46*, 2814–2823.
- (9) Barboiu, M. *Angew. Chem., Int. Ed.* **2012**, *51*, 11674–11676.
- (10) Barboiu, M.; Le Duc, Y.; Gilles, A.; Cazade, P.-A.; Michau, M.; Legrand, Y.-M.; van der Lee, A.; Coasne, B.; Paivizi, P.; Post, J.; Fyles, T. *Nat. Commun.* **2014**, *5*, 4142.
- (11) Le Duc, Y.; Michau, M.; Gilles, A.; Gence, V.; Legrand, Y.-M.; van der Lee, A.; Tingry, S.; Barboiu, M. *Angew. Chem., Int. Ed.* **2011**, *50* (48), 11366–11372.
- (12) Berezin, S. K.; Davis, J. T. *J. Am. Chem. Soc.* **2009**, *131*, 2458–2459.
- (13) Otis, F.; Auger, M.; Voyer, N. *Acc. Chem. Res.* **2013**, *46*, 2934–2943.
- (14) Gokel, G. W.; Negin, S. *Adv. Drug Delivery Rev.* **2012**, *64*, 784–796.
- (15) Bong, D. T.; Clark, T. D.; Granja, J. R.; Ghadiri, M. R. *Angew. Chem., Int. Ed.* **2001**, *40*, 988.
- (16) Weiss, L. A.; Sakai, N.; Ghebremariam, B.; Ni, C.; Matile, S. *J. Am. Chem. Soc.* **1997**, *119*, 12142.
- (17) Goto, C.; Yamamura, M.; Satake, A.; Kobuke, Y. *J. Am. Chem. Soc.* **2001**, *123*, 12152–12153.

- (18) Eggers, P. K.; Fyles, T. M.; Mitchell, K. D. D.; Sutherland, T. J. *Org. Chem.* **2003**, *68*, 1050–1058.
- (19) Cazacu, A.; Tong, C.; van der Lee, A.; Fyles, T. M. M. *J. Am. Chem. Soc.* **2006**, *128*, 9541–9548.
- (20) Matile, S.; Sakai, N. In *Analytical Methods in Supramolecular Chemistry*; Schalley, C. A., Ed. Wiley-VCH: Weinheim, 2007; pp 381–418.
- (21) Eisenmann, G.; Horn, R. *J. Membr. Biol.* **1983**, *76*, 197–225.
- (22) Winum, J.-Y.; Matile, S. *J. Am. Chem. Soc.* **1999**, *121*, 7961–7962.
- (23) Woolley, G. A.; Kapral, M. K.; Deber, C. M. *FEBS Lett.* **1987**, *224*, 337–342.
- (24) Barboiu, M.; Vaughan, G.; van der Lee, A. *Org. Lett.* **2003**, *5*, 3073.
- (25) Barboiu, M. *J. Inclusion Phenom. Mol. Recognit. Chem.* **2004**, *49*, 133–137.
- (26) (a) Legrand, Y.-M.; Barboiu, M. *Chem. Rec.* **2013**, *13*, 524.
(b) Barboiu, M.; Cerneaux, S.; van der Lee, A.; Vaughan, G. *J. Am. Chem. Soc.* **2004**, *126*, 3545–3550.
- (27) Mihai, S.; Cazacu, A.; Arnal-Herault, C.; Nasr, G.; Meffre, A.; van der Lee, A.; Barboiu, M. *New J. Chem.* **2009**, *33*, 2335.
- (28) Cazacu, A.; Legrand, Y. M.; Pasc, A.; Nasr, G.; Van der Lee, A.; Mahon, E.; Barboiu, M. *Proc. Natl. Acad. Sci. U. S. A.* **2009**, *106*, 8117.
- (29) MacKinnon, R. *Angew. Chem., Int. Ed.* **2004**, *43*, 4265–4277.
- (30) Alexandratos, S. D.; Stine, C. L. *React. Funct. Polym.* **2004**, *60*, 3–16.
- (31) Kado, S.; Takeshima, Y.; Nakahara, Y.; Kimura, K. *J. Inclusion Phenom. Mol. Recognit. Chem.* **2012**, *72*, 227–232.
- (32) Yu, H.-R.; Hu, J.-Q.; Lu, X.-H.; Ju, X.-J.; Liu, Z.; Rui Xie, R.; Wang, W.; Chu, L. Y. *J. Phys. Chem. B* **2015**, *119*, 1696–1705.
- (33) Otis, F.; Racine-Berthiaume, C.; Voyer, N. *J. Am. Chem. Soc.* **2011**, *133*, 6481–6483.
- (34) Sun, Z.; Barboiu, M.; Legrand, Y.-M.; Petit, E.; Rotaru, A. *Angew. Chem., Int. Ed.* **2015**, *54*, 14473–14477.
- (35) Sun, Z.; Gilles, A.; Kocsis, I.; Legrand, Y.-M.; Petit, E.; Barboiu, M. *Chem.—Eur. J.* **2015**, DOI: 10.1002/chem.201503979.